Fast and Slow Contrast Adaptation in Retinal Circuitry

Stephen A. Baccus[1] and Markus Meister
Department of Molecular and Cellular Biology
Harvard University
16 Divinity Avenue
Cambridge, Massachusetts 02138

Summary

The visual system adapts to the magnitude of intensity fluctuations, and this process begins in the retina. Following the switch from a low-contrast environment to one of high contrast, ganglion cell sensitivity declines in two distinct phases: a fast change occurs in <0.1 s, and a slow decrease over ~10 s. To examine where these modulations arise, we recorded intracellularly from every major cell type in the salamander retina. Certain bipolar and amacrine cells, and all ganglion cells, adapted to contrast. Generally, these neurons showed both fast and slow adaptation. Fast effects of a contrast increase included accelerated kinetics, decreased sensitivity, and a depolarization of the baseline membrane potential. Slow adaptation did not affect kinetics, but produced a gradual hyperpolarization. This hyperpolarization can account for slow adaptation in the spiking output of ganglion cells.

Introduction

Vision operates under a wide range of environmental conditions. Since individual neurons can represent only a limited range of signals with their range of membrane potentials, the system must somehow adapt its sensitivity to the current range of light intensities in each environment. This adaptation alters the rules by which a neuron responds to sensory input. For example, following a decrease in the average light intensity, the visual system's adaptations include pupil dilation, increased amplification in the phototransduction cascade (Pugh et al., 1999), diminished ganglion cell receptive field surrounds (Barlow and Levick, 1969), slower ganglion cell responses (Enroth-Cugell and Lennie, 1975), and changes in cortical processing (Yang and Stevenson, 1999). This collection of adjustments improves visual performance at the new mean light level.

The visual system also adapts its performance to the range of intensity fluctuations about the mean, called the contrast. In a high-contrast environment, retinal ganglion cells are much less sensitive than in a low-contrast environment (Sakai et al., 1995; Shapley and Victor, 1978). Some of this adjustment of retinal sensitivity is essentially instantaneous, occurring within <0.1 s of the contrast change and well within the immediate response time of the retina (Victor, 1987). More recently, another component of modulation was found that adapts retinal sensitivity much more slowly, on the scale of 1–10 s (Chander and Chichilnisky, 2001; Smirnakis et al., 1997).

This seems to occur at multiple sites within the retinal circuit, beginning in bipolar cells (Brown and Masland, 2001; Rieke, 2001) and including intrinsic properties of ganglion cells (Kim and Rieke, 2001).

The fast and slow components clearly play different roles for vision, and are almost certainly produced by different mechanisms. Fast adaptation, also called "contrast gain control," affects the moment-to-moment response of the retina (Victor, 1987). For example, it can prevent saturation of the retinal output as the eye scans over reflection highlights in the scene or across sharp shadow edges. Fast adaptation also has a profound effect on how the retina processes moving stimuli (Berry et al., 1999). Slow contrast adaptation, on the other hand, takes place over many seconds, during which time the animal performs many eye or head movements that scan the scene. As a result, this prolonged modulation adjusts retinal sensitivity to the overall contrast level in the scene, which may vary with conditions of illumination (indirect light scattered through clouds versus direct light from the sun) or the physical environment (golf course versus pages of printed text). Such slow adjustments are well documented in human psychophysics (Blakemore and Campbell, 1969; Greenlee et al., 1991) and in cortical neurons (Ohzawa et al., 1985), and our retina probably contributes substantially to this process (Chander and Chichilnisky, 2001; Truchard et al., 2000).

On this background, it is important to separate these two different contrast-dependent processes: which aspects of retinal processing are modified quickly, and which by the slow contrast adaptation? Previous studies have focused on characterizing retinal processing in the steady state, well after a contrast transition (Chander and Chichilnisky, 2001; Kim and Rieke, 2001; Rieke, 2001; Sakai et al., 1995; Shapley and Victor, 1978), thus conflating the slow and the fast modulations. Here, we resolve this ambiguity by analyzing the visual response properties of the retina systematically at different times following a change in the stimulus contrast. We measured fast adaptation by comparing response properties immediately before and after a change in contrast, and slow adaptation by comparing response properties at different times within the same contrast environment. Moreover, we performed this analysis on recordings from every major neuron type in the retina. The results reveal the nature of the fast and slow changes and point to where they arise within the retinal circuit.

Results

Modulations of the Retinal Light Response
We first describe the approach for probing retinal light responses. The stimulus was a rapidly flickering uniform field whose light intensity changed randomly every 30 ms with a Gaussian distribution about the mean. On a much longer time scale, every 30 s, we alternated the contrast of the flicker—the width of the Gaussian distribution—between a low and a high value. Then we analyzed how the light response changed over time following the switch to the new contrast environment.

[1]Correspondence: baccus@fas.harvard.edu

Repeated flicker stimulus

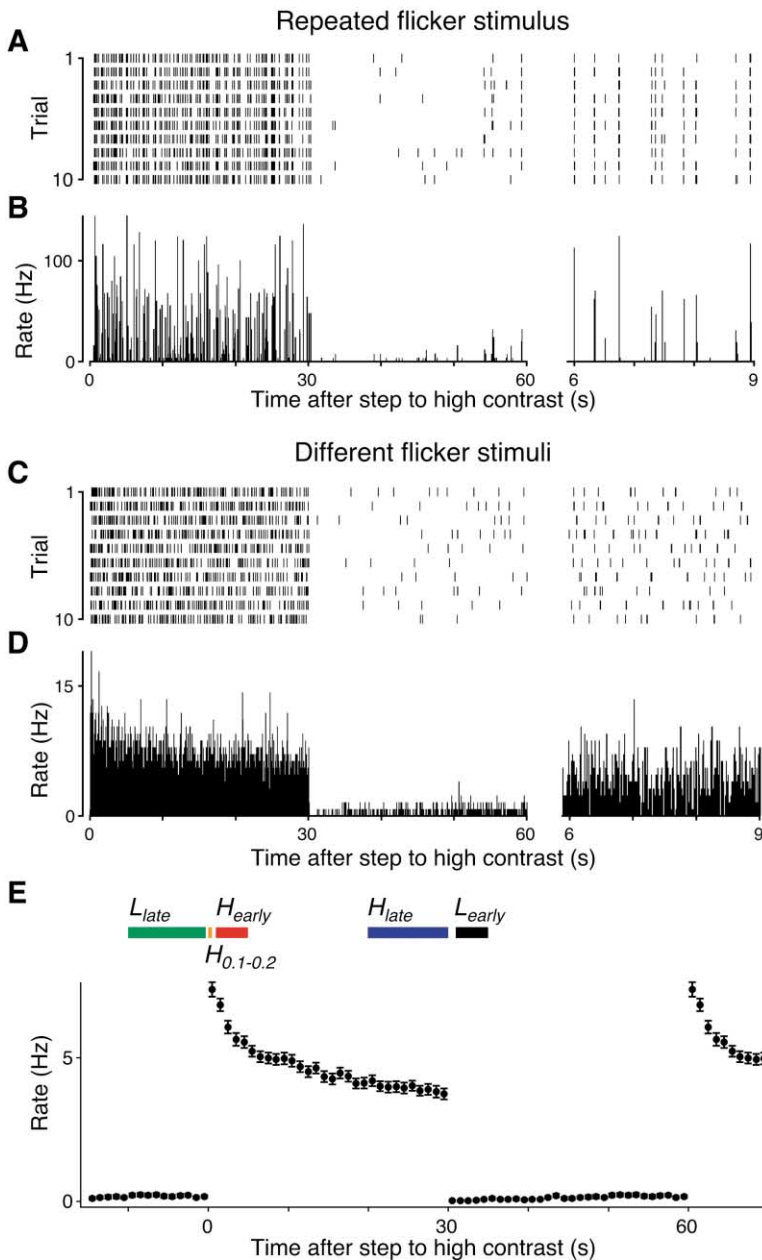
Different flicker stimuli

Figure 1. Salamander Ganglion Cell Responses Modulated by Changes in Contrast

Each 60 s stimulus trial contained 30 s of random flicker at high contrast followed by 30 s at low contrast; the mean intensity remained constant throughout. Subsequent trials either repeated the identical flicker sequence (A and B), or presented a different flicker sequence each time (C–E).
(A) Raster plot of spikes from a "fast OFF" (Warland et al., 1997) ganglion cell in response to the repeating stimulus. At right is an expanded time scale.
(B) Peristimulus time histogram (PSTH) of the response to 15 stimulus repeats, calculated with 15 ms bins.
(C) Raster plot for trials with different stimuli.
(D) PSTH for 84 trials with different stimuli, calculated with 15 ms bins.
(E) Same as (D), but using 1 s bins, smoothing over the rapid firing rate variations. Bars define the various time periods surrounding the contrast switch used to analyze responses. Note time scale is different from (A)–(D).

To inspect the output of the retina under these conditions, the spike trains of multiple ganglion cells were recorded with an electrode array (Figure 1). During any given episode of flicker, the ganglion cell produced a sequence of brief firing events in which the spike rate varied up and down very rapidly and reproducibly across repeated trials (Figures 1A and 1B) (Berry et al., 1997). Within a given contrast environment, this light response depended only on the immediate history of the flicker stimulus, extending about 0.2 s into the past (Figure 2A) (Keat et al., 2001). One would like to know how the rules that govern this immediate light response change as a result of a switch in contrast.

One simple indication for a change in the immediate light response comes from inspecting the cell's average firing rate, measured using many different flicker sequences (Figure 1C). This average rate declined gradually with time in the high-contrast condition and recovered gradually during low contrast (Figures 1D and 1E). These changes occurred over many seconds, a period 10–100 times longer than the 0.2 s integration time of the immediate light response. Because of this difference in time scales, one can distinguish the immediate neural code of the ganglion cell, by which it reports the preceding 0.2 s of stimulation with a firing rate modulation of >100 Hz (Figures 1A and 1B), from the gradual adjustments of that code by slow contrast adaptation (Figures 1C–1E).

The average firing rate has served as a useful measure of slow contrast adaptation (Brown and Masland, 2001; Smirnakis et al., 1997), but by itself says little about how the neuron encodes the stimulus. For example, does
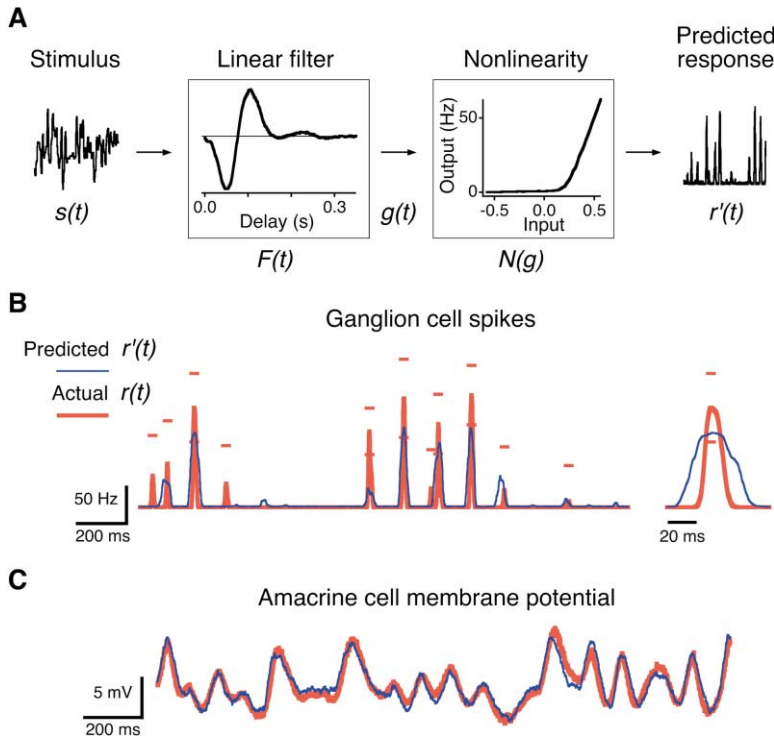
A

Stimulus   Linear filter   Nonlinearity   Predicted response

$s(t)$ $F(t)$ $N(g)$ $r'(t)$

$g(t)$

B

Ganglion cell spikes

Predicted $r'(t)$

Actual $r(t)$

50 Hz

200 ms

20 ms

C

Amacrine cell membrane potential

5 mV

200 ms

Figure 2. LN Descriptions of Neural Responses

(A) The LN model to predict the firing rate of a "fast OFF" ganglion cell. The flicker stimulus $s(t)$ is convolved with a linear filter $F(t)$, and then the result $g(t)$ is passed through a fixed nonlinearity $N(g)$ to produce the predicted firing rate $r'(t)$.

(B) Predicted firing rate $r'(t)$ compared to the actual response $r(t)$. Error intervals indicate the standard deviation across trials at the peaks of firing events. Right, one firing event on an expanded time scale. For eight ganglion cells analyzed in this way, the normalized rms difference (see Experimental Procedures) between the predicted and actual firing rate, 0.28 ± 0.02 (mean $\pm$ SEM), was almost as small as the rms difference between actual responses to a repeated stimulus, 0.24 ± 0.03.

(C) The LN prediction of an amacrine cell membrane potential compared to the actual response. Segments displayed in (B) and (C) are representative of the entire recording.

the average rate decline because there are different firing events or because each firing event produces fewer spikes?

Light Responses Can Be Described by an LN Model

To determine what features of the flicker stimulus excite a given neuron, and how sensitively it responds to those events, we summarized the light response of ganglion cells and other retinal neurons using an LN ("linear-nonlinear") model (Berry and Meister, 1998; Chichilnisky, 2001; Hunter and Korenberg, 1986; Kim and Rieke, 2001; Rieke, 2001; Sakai et al., 1988). In this scheme (Figure 2A), the stimulus waveform $s(t)$ is passed through a linear temporal filter $F(t)$, and the result $g(t)$ is transformed by a nonlinear function $N(g)$ to the model's response $r'(t)$. The filter $F(t)$ and the nonlinearity $N(g)$ are computed so the prediction of the model $r'(t)$ matches the measured neural response $r(t)$ as closely as possible (see Experimental Procedures). Thus, the linear filter summarizes the temporal processing between the stimulus and the neuron's response, whereas the nonlinearity describes the instantaneous relationship between the filtered stimulus and the response. An intuitive description of the LN model is that the time-reverse of the filter function $F(t)$ represents the stimulus feature to which this neuron is most sensitive. The filtered stimulus $g(t)$ measures how strongly that feature is represented in the current stimulus, and the function $N(g)$ determines how $g(t)$ is transformed into a response, including threshold effects, rectification, and other distortions.

The LN model used to fit a ganglion cell's firing rate is illustrated in Figures 2A and 2B. The filter function $F(t)$ was biphasic, with a negative first peak, indicating that this neuron was excited by OFF-type transients in

the flicker stimulus. For times >0.2 s, the filter vanished, indicating that the cell responded only to the preceding 0.2 s of stimulation. The nonlinearity $N(g)$ had a sharp threshold. At low input values, the output firing rate was close to zero, showing that this neuron was nearly silent during ON-type stimulus transients or weak OFF-type transients. Above a certain threshold, the firing rate increased linearly with the strength of the stimulus. The prediction of this model produced a good fit to the neuron's actual firing rate (Figure 2B). Most of the firing events were well matched in their amplitude and timing, although the actual events were somewhat narrower than the predictions (Figure 2B, right). This aspect can be improved with a more intricate model of retinal signaling (Keat et al., 2001), but that is not essential for the present purpose of assessing temporal processing and sensitivity. The LN fit was also applied to membrane potential recordings from other retinal neurons. In almost all cases, this produced a very good match between predicted and actual responses: the rms difference between the predicted and actual response was similar or less than the variability of the cell's response across identical trials (Figure 2C) (Kim and Rieke, 2001; Rieke, 2001).

Step Changes in Contrast Trigger Fast and Slow Changes in Retinal Output

To analyze the time course of modulation of a neuron's light response, LN models were computed separately for various time intervals before and after the contrast switch (Figure 1E): H_{early}, 1–5 s after a step to high contrast; H_{late}, 20–30 s after a high-contrast step; L_{early}, 1–5 s after a low-contrast step; and L_{late}, 20–30 s after a low-contrast step. Using these time periods, Figure 3 shows the effects of a contrast step on ganglion cell firing.
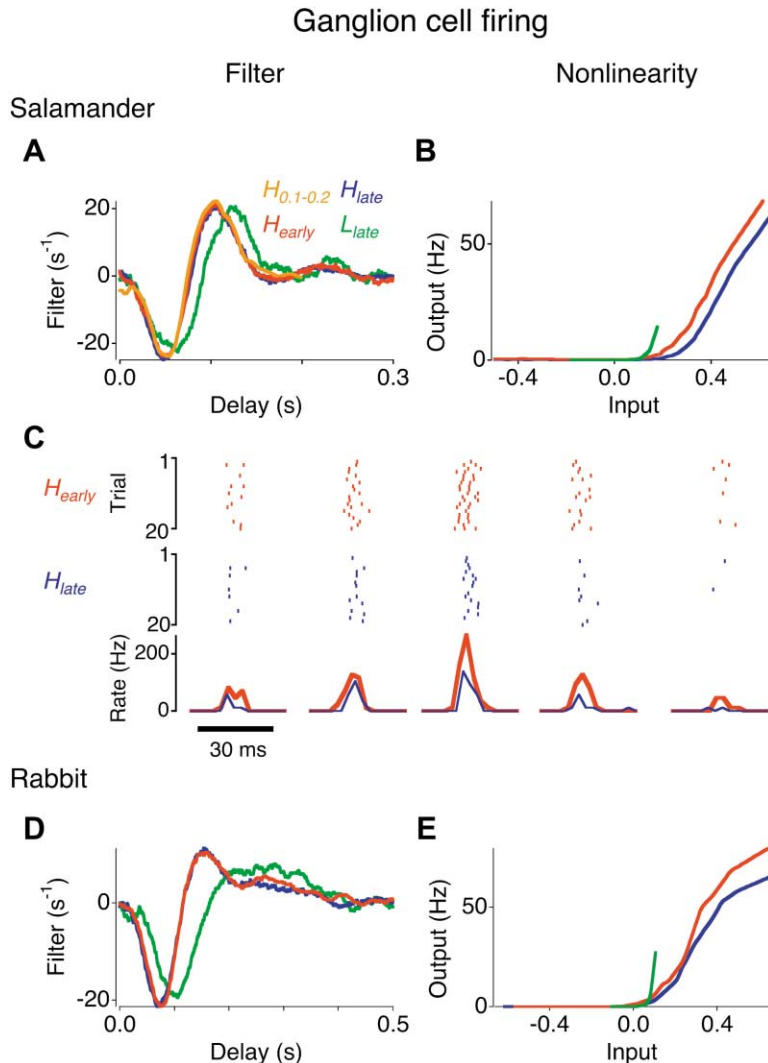
Ganglion cell firing

Figure 3. LN Models of Ganglion Cell Firing during Contrast Adaptation in Salamander and Rabbit Retina

(A) Linear filter for a salamander ganglion cell during the time periods H_{early}, H_{late}, and L_{late} (defined in Figure 1E). To test how rapidly the filter function changed, we also performed a fit over the time interval $H_{0.1-0.2}$, 0.1–0.2 s after the high-contrast step to yield a filter 0.2 s in duration. Note the curves for H_{early} and H_{late} are partly obscured by $H_{0.1-0.2}$. Filters are normalized to have equal variance (see Experimental Procedures).

(B) Nonlinearity during H_{early}, H_{late}, and L_{late}. Average firing rate during H_{late} was 4 Hz.

(C) Raster plot and PSTH of representative firing events of a salamander ganglion cell responding to the same 3 s stimulus sequence repeated during H_{early} and H_{late}. PSTH is calculated from 30 trials with 3 ms bins.

(D and E) Filter and nonlinearity for a rabbit ganglion cell during H_{early}, H_{late}, and L_{late}, displayed as in (A) and (B). Average rate during H_{late} was 9 Hz.

Comparing the response directly before (L_{late}) and after (H_{early}) the switch to high contrast, the time course of the temporal filter became significantly faster. The change in the filter kinetics was complete within 0.2 s of the contrast switch, as soon as it could be measured (see $H_{0.1-0.2}$ in Figure 3A). The normalized rms difference (see Experimental Procedures) between the filters for L_{late} and H_{early} was 0.82 ± 0.13 (mean ± SD, 10 cells) in the salamander, and 0.89 ± 0.27 (11 cells) in the rabbit retina. At the same time, the nonlinearity shifted to a much higher threshold, such that the range of input values that was effective at firing the cell during L_{late} produced virtually no activity during H_{early}. Thus, at high contrast, these ganglion cells responded more quickly but with lower average sensitivity (specifically, we define "sensitivity" as the average slope of the nonlinearity across a given range of input values). This fast adaptation occurs on the same time scale as the immediate light response, within the integration time of the filter $F(t)$ (Victor, 1987).

Further changes in sensitivity occurred on a long time scale. Comparing H_{early} and H_{late}, the threshold nonlinearity moved further to the right, so the cell's response

became even less sensitive. However, the time course of the filter function remained unchanged over this period. In contrast to the large change in filters seen between L_{late} and H_{early}, the filters for H_{early} and H_{late} differed by an rms measure of only 0.11 ± 0.06 (mean ± SD, 10 cells) in the salamander, and 0.13 ± 0.06 (11 cells) in the rabbit. The size of this small discrepancy was below the resolution of the method, since similar differences were present between two independent measurements during H_{late} (0.10 ± 0.03 in the salamander, 0.14 ± 0.07 in the rabbit).

Thus, a switch to high contrast triggers two changes in the retinal output. Immediately after the switch, fast adaptation makes the ganglion cell response faster and less sensitive. Over the following 5–30 s, slow adaptation leads to a further decline in sensitivity without any change in temporal processing. Therefore, the gradual decline in the average firing rate (Figure 1E) results because fewer spikes are generated in each firing event, rather than a change in when firing events are produced. This conclusion based on examination of LN models was confirmed explicitly by repeating the same flicker stimulus sequence during H_{early} and during H_{late} (Figure

Filter | Nonlinearity
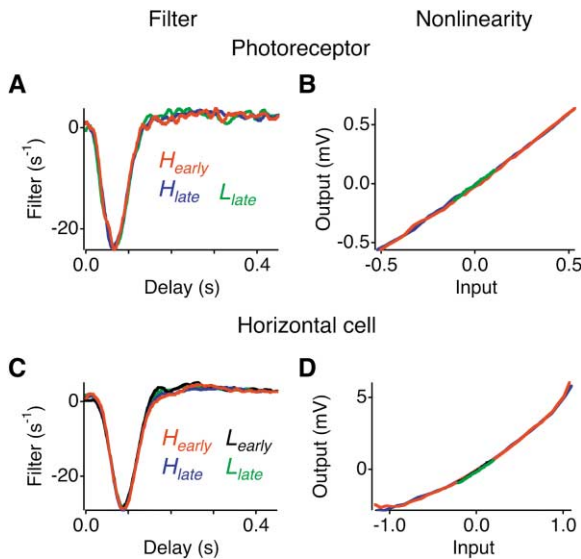
Photoreceptor

Horizontal cell

Figure 4. Responses of Outer Retinal Neurons during Contrast Adaptation

LN models of intracellularly recorded membrane potentials for a cone photoreceptor (A and B) and a horizontal cell (C and D), displayed as in Figure 2. Resting potentials (V_{rest}) were −41mV (photoreceptor) and −44mV (horizontal cell). The time periods H_{early}, H_{late}, L_{early}, and L_{late} are defined in Figure 1E. Note that the trace for H_{late} is partly obscured by H_{early}.

3C). Slow adaptation did not change the time of firing events, but did decrease the number of spikes in each event.

Fast and Slow Contrast Adaptation Originate in the Inner Retina

To determine where these changes occurred within the circuitry, we analyzed intracellular membrane potential recordings from individual neurons of the salamander retina. Cone photoreceptors (Figures 4A and 4B) had a very simple light response to these flicker stimuli. The filter function $F(t)$ was dominated by a single OFF-type peak, and the nonlinearity $N(g)$ was in fact linear to very good approximation. Most importantly, there was no detectable change in these parameters induced by the contrast switch, neither during the immediate transition from low to high contrast, nor in the subsequent adaptation period at high contrast, even though ganglion cells recorded simultaneously did slowly adapt (data not shown). The filters during H_{early} and H_{late} had an rms difference of less than 0.05, as did the nonlinearities (six cells). Thus, cones do not participate in fast or slow contrast adaptation.

Horizontal cell responses were also characterized by an almost monophasic OFF-type filter function (Figures 4C and 4D), and had a larger amplitude, or voltage gain, than did photoreceptors (Baylor et al., 1971; Yang and Wu, 1996). The function $N(g)$ showed an expansive nonlinearity, meaning that the slope increased toward positive input values. As in photoreceptors, these parameters of the light response were indistinguishable at low and high contrast.

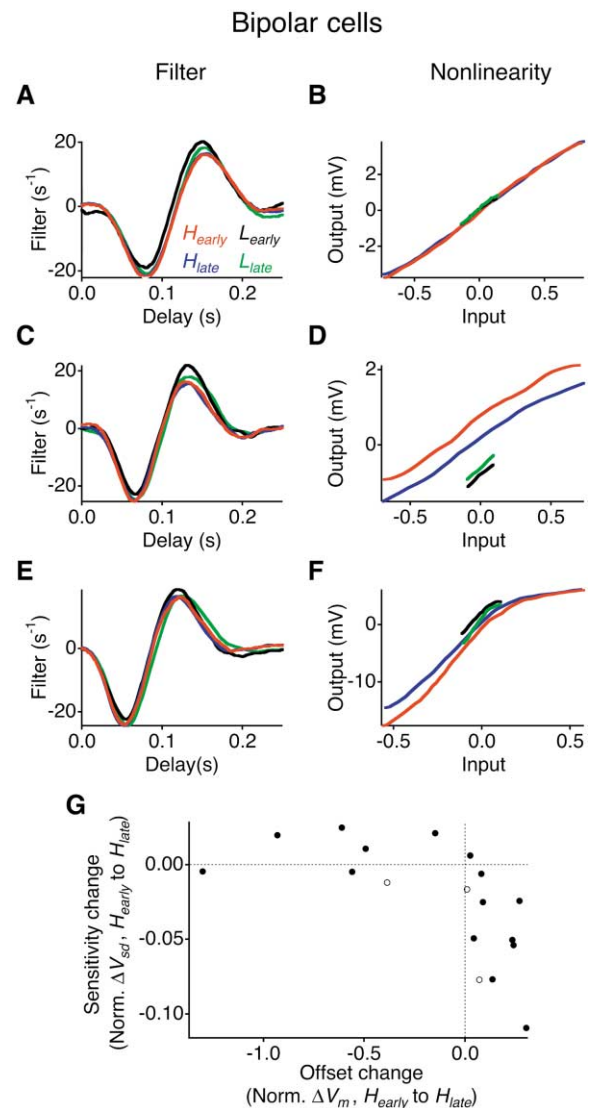Bipolar cells had strongly biphasic filters, indicative

Bipolar cells

Filter | Nonlinearity

Figure 5. Different Properties of Fast and Slow Adaptation in Bipolar Cells

(A–F) Filters and nonlinearities for bipolar cells during H_{early}, H_{late}, L_{early}, and L_{late}, displayed as in Figure 2. Note that some traces H_{late} are partly obscured by the H_{early} traces. (A and B) Cell with no slow adaptation to contrast ($V_{rest} = -38$mV). (C and D) Cell that adapted to contrast by changes in the average membrane potential ($V_{rest} = -45$mV). (E and F) Cell that adapted to contrast by changes in the slope of the nonlinearity ($V_{rest} = -40$mV).

(G) The effects of slow contrast adaptation between H_{early} and H_{late} for 18 bipolar cells. The fractional change in the standard deviation of the membrane potential (V_{sd}) is plotted against the change in average membrane potential. Both numbers are normalized to V_{sd} during H_{late}. V_{sd} during high contrast was 1.4 ± 0.1mV (mean ± SEM, n = 18) and the peak-to-peak response amplitude was 7 ± 1mV. Filled circles are OFF cells; open circles are ON cells.

of high-pass filtering at the photoreceptor synapse (Figures 5A, 5C, and 5E). In OFF-type bipolar cells, this filter function showed a small but significant change in the time to peak between low and high contrast (Rieke, 2001). As in ganglion cells (Figure 3A), this change was instantaneous following the contrast switch: the time to peak during H_{early} was 0.93 ± 0.01 (mean ± SEM, n = 15)

times that during L_{late}. During adaptation to high contrast between H_{early} and H_{late}, the filter shape remained unaltered.

In the nonlinearity of bipolar cells, we found three types of contrast dependence. In some cells, no significant changes occurred either between L_{late} and H_{early} or between H_{early} and H_{late} (Figure 5B). In other cells, immediately after the transition to high contrast, the function $N(g)$ shifted to positive potentials (Figure 5D). During the subsequent adaptation period, it slowly hyperpolarized again until it almost matched the steady-state behavior under low-contrast conditions. Following a transition to low contrast, the opposite changes took place: an immediate hyperpolarizing shift, followed by a gradual depolarization. The third behavior was a change in the slope of the nonlinearity, which became shallower during adaptation between H_{early} and H_{late} (Figure 5F). Except for this change in sensitivity, the shape of the nonlinearity remained the same.

To further examine these distinct adaptation behaviors across the bipolar cell population, we returned to the membrane potential recordings during high contrast. For each cell, we measured the change in the average membrane potential between H_{early} and H_{late}, to capture the vertical shift exemplified in Figure 5D and also the change in the standard deviation of the membrane potential, which captures the slope change in Figure 5F. Bipolar cells varied in their degree of slow adaptation to high contrast. However, each individual cell showed either a membrane potential offset or a change in sensitivity, but not both (Figure 5G). Apparently these are distinct modes of slow contrast adaptation, perhaps restricted to different bipolar cell subtypes.

Most of the amacrine cells examined (18 of 26) showed no contrast-dependent changes in the light response: the LN models computed at low and high contrast overlaid almost perfectly (Figures 6B and 6C). Amacrine cells are a diverse class of neurons, as judged by their receptive fields, responses to light flashes, cell morphology, and neuropeptide expression (MacNeil et al., 1999; Yang et al., 1991). We found nonadapting amacrine cells in several different cell types. All sustained OFF-type amacrine cells (14 of 14) showed no contrast-dependent adaptation (Figures 6A–6C, rows 1 and 2). Some transient amacrine cells also did not adapt (Figures 6A–6C, row 3). The dendritic arborizations of nonadapting amacrines ranged from wide fields to rather narrow fields (Figure 6D).

A subset of amacrine cells (8 out of 26) was strongly modulated by the contrast level (Figures 6E–6G). Most conspicuous were the effects on the nonlinearity (Figure 6G). After the transition to high contrast, cells depolarized rapidly between L_{late} and H_{early} (1.25 $\pm$ 0.19mV, mean $\pm$ SEM), then hyperpolarized slowly between H_{early} and H_{late} (-0.75 ± 0.13mV). When contrast decreased, cells hyperpolarized rapidly, then depolarized slowly (Figures 6G and 6H). For some neurons (Figure 6F, row 1) the temporal filter $F(t)$ changed to a faster time course at high contrast, without any subsequent slow changes. Note this parallels the behavior seen in adapting bipolar cells (Figure 5), although the change in the filter was greater in amacrine cells. The primary effect of slow contrast adaptation was a gradual change in the cell's average membrane potential without changes in tempo-

ral processing. Amacrine cells that showed such adaptation included all neurons with ON-OFF flash responses (six of six such cells, e.g., Figures 6E–6G, row 1).

Slow Contrast Adaptation of Ganglion Cell Firing Results from Shifts in the Baseline Potential

The subthreshold membrane potential responses of retinal ganglion cells were also modulated by the contrast level. Immediately following a switch to high contrast, the filter changed to a faster time course (Figure 7A). As in adapting bipolar and amacrine cells, the cell depolarized rapidly, as indicated by the nonlinearity. In some ganglion cells, there was also a rapid change in the shape of the nonlinearity, which became shallower at high contrast (Figure 7B, row 2).

During the subsequent period of slow adaptation, the filter remained unchanged. The nonlinearity gradually became more negative (by -1.0 ± 0.2mV, nine cells) (Figures 7B and 7C), but retained the same general shape (Figure 7B, row 2). In some cases, the nonlinearity was slightly steeper during H_{late} than H_{early} (Figure 7B). This might be due to a slight increase in the driving force of excitatory conductances at the more hyperpolarized potential. Over this period of progressive hyperpolarization, the ganglion cell's firing rate declined, and the two effects followed the same time course (Figure 7D). This suggests that the slow hyperpolarization of the nonlinearity $N(g)$ can account for the effects of slow contrast adaptation on ganglion cell firing.

We tested directly whether a steady change in the ganglion cell membrane potential could mimic the effects of slow contrast adaptation (Figure 8). Spiking responses to a flicker stimulus were recorded intracellularly; then we injected hyperpolarizing current that lowered the cell's resting potential by several millivolts and repeated the same stimulus. During this current injection, subthreshold membrane potential fluctuations were similar to the control case (Figure 8A). Due to the negative offset, they elicited approximately 20% fewer spikes, but those occurred at nearly the same times as in the preceding trial without current. The LN models of ganglion cell firing under the two conditions confirmed that steady current did not alter the linear filter, but simply moved the nonlinearity to the right (n = 5, Figures 8B and 8C), mirroring the effects of slow contrast adaptation (Figures 3A and 3B).

Discussion

The goal of this work was to dissect how the stimulus contrast modulates visual response properties throughout the retina, distinguishing the rapid from the slow components of contrast adaptation. The principal results are: (1) contrast-dependent changes occur in certain bipolar cells, certain amacrine cells, and all ganglion cells. (2) Neurons that undergo a fast change in any response property also experience a subsequent slow change and vice versa. (3) The fast effect involves a change in the kinetics of the light response, a shift in the baseline membrane potential, and sometimes a change in the sensitivity. (4) The slow change is primarily a shift in the baseline membrane potential and invariably opposes the membrane polarization that occurred dur-
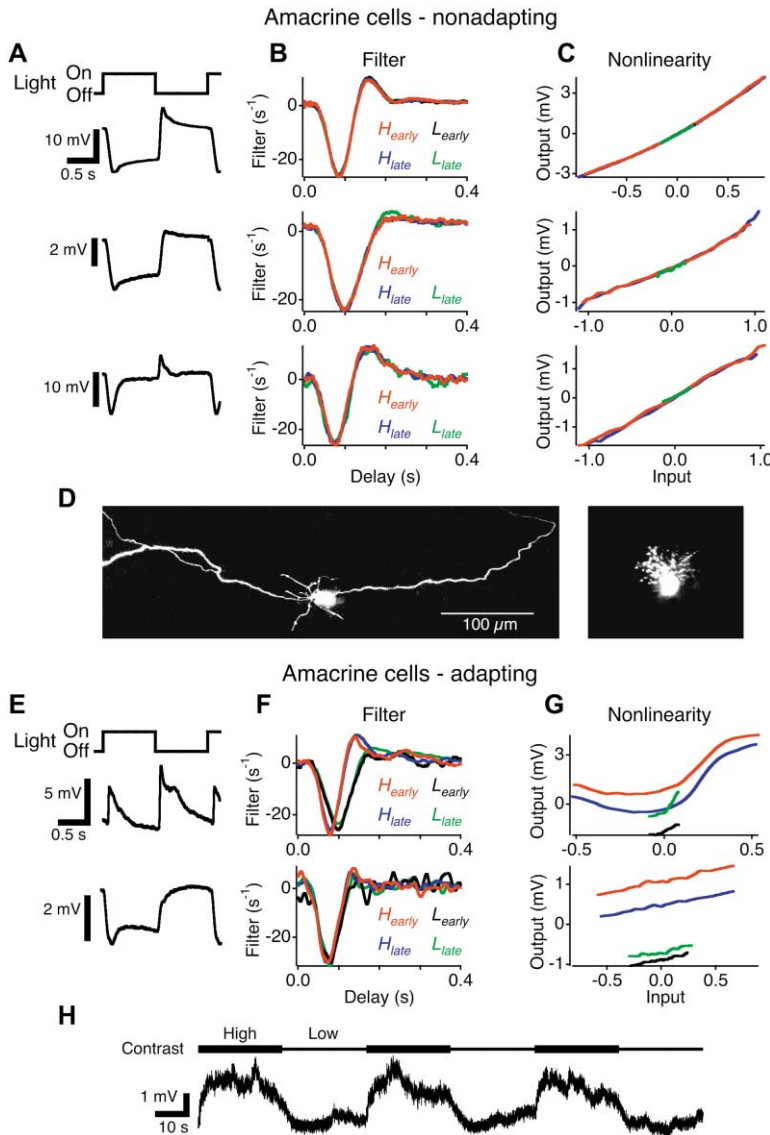
Figure 6. Some Amacrine Cells Change Their Baseline Membrane Potential during Contrast Adaptation

(A–D) Amacrine cells that did not adapt to contrast. (A) Responses of three amacrine cells to full-field flashes of 100% contrast, averaged over 15 trials. (B and C) Filters and nonlinearities for these cells during H_{early}, H_{late}, L_{early}, and L_{late}, displayed as in Figure 2. Note the H_{late} trace is partly obscured by the H_{early} trace. $V_{rest} = -55$mV (row 1), -65mV (row 2), -65mV (row3). (D) Vertical projections of confocal images taken of two nonadapting amacrine cells; both had sustained flash responses (data not shown).

(E–H) Amacrine cells that adapted to contrast. (E) Responses of two amacrine cells to full-field flashes of 100% contrast, averaged over 15 trials. (F and G) Filters and nonlinearities for these cells during H_{early}, H_{late}, L_{early} and L_{late}. $V_{rest} = -53$mV (row 1), -50mV (row 2). (H) Membrane potential of an amacrine cell (bottom panel in E–G) during step changes in contrast. On this slow time scale, the immediate light response to the flicker cannot be resolved, but the modulations of the baseline potential are apparent.

ing the fast phase. (5) In ganglion cells, the slow hyperpolarization can account for slow contrast adaptation of the spiking output.

The Immediate Effects of a Contrast Change

In cones and horizontal cells, a substantial change in stimulus contrast had no detectable effect on response properties, in good accordance with prior reports on the steady-state behavior of these neurons (Rieke, 2001; Sakai and Naka, 1987). This eliminates one possible explanation for contrast adaptation, namely that it relies on the mechanisms of light adaptation in the cone's transduction cascade, triggered preferentially at high contrast by larger stimulus transients.

Fast adaptation is first seen in bipolar cells. The immediate effects of a contrast increase include a change in the kinetics of the filter $F(t)$ and sometimes a change in the slope of the nonlinearity $N(g)$ (Rieke, 2001), or a depolarizing shift of $N(g)$ (Figures 5 and 9). Still other bipolar cells have nonlinear properties that are not influ-

enced at all by a contrast change. This diversity likely reflects the wide range of morphological and functional subtypes among bipolar cells (Wu et al., 2000).

Because the depolarizing shift is seen only in certain bipolar cells and not in horizontal cells, it is probably not caused by changes in transmitter release from the photoreceptor. Candidate mechanisms include a conductance in the bipolar cell membrane that is activated only at depolarized potentials or at high concentration of neurotransmitter. However, to account for the depolarizing shift in the nonlinearity over the entire range of input values (Figure 5D), the effects of this conductance must last longer than the typical fluctuation in the cell's input, namely the 0.2 s duration of the filter $F(t)$.

The rapid change in kinetics along with a steady depolarization are also seen in certain amacrine types (Figures 6 and 9) and all ganglion cells (Figures 7 and 9). In some of these neurons an additional immediate change is apparent: the nonlinearity becomes substantially shallower at high contrast, indicating a fast reduction of
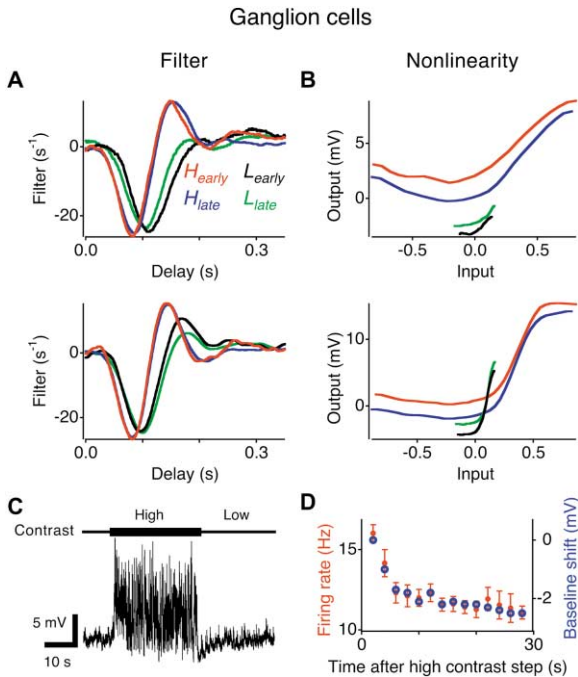
Ganglion cells

Figure 7. Ganglion Cell Voltage Responses Are Modulated by Contrast

(A and B) Filters and nonlinearities of two ganglion cells during H_{early}, H_{late}, L_{early}, and L_{late}, displayed as in Figure 2. $V_{rest} = -71mV$ (row 1), $-68mV$ (row 2).

(C) Membrane potential of a ganglion cell (upper panels in [A] and [B]) during one stimulus trial with high and low contrast. Spikes were removed from the trace (see Experimental Procedures).

(D) The average firing rate (filled circles) and membrane potential baseline shift (open circles) measured for the same ganglion cell in 2 s time bins following the high-contrast step. The baseline shift was calculated as the vertical shift between the nonlinearity for that time bin and the nonlinearity in the first bin.
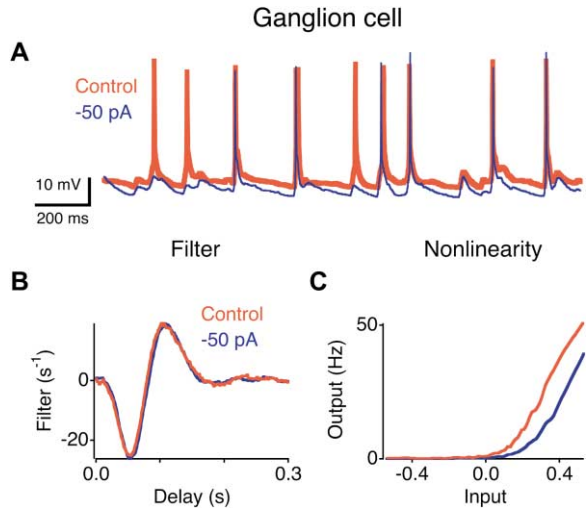
Ganglion cell

Figure 8. Steady Current Injection into Ganglion Cells Mimics Slow Contrast Adaptation

(A) Ganglion cell membrane potential in response to a high-contrast stimulus with and without -50 pA current injected into the cell. $V_{rest} = -64mV$.

(B and C) Filter and nonlinearity computed for the spiking response under the two conditions.

sensitivity (Figures 6G, 7B, and 9). In some cases, this amounts to a lateral scaling of the nonlinearity; proportionally greater excursions of the stimulus are required to elicit the same voltage response. This could be understood as a consequence of shunting inhibition from other amacrine cells. At high contrast, the amacrine cell responses are stronger (Figure 6) and will drive a greater shunting conductance, either pre- or postsynaptically, thus scaling down the excitatory input from bipolar cells. An alternative is that an intrinsic conductance in amacrine and ganglion cells quickly changes the membrane conductance upon a change in contrast.

Previous work examining the steady-state responses of bipolar and ganglion cells suggested that the nonlinearity at different contrast levels is identical except for a scaling along the abscissa. In that case, the retina would respond as though the high-contrast stimulus were scaled down by some gain factor (Chander and Chichilnisky, 2001; Kim and Rieke, 2001; Rieke, 2001). While this may be a reasonable approximation at steady state, it is not true immediately after the contrast switch (Figures 3, 5–7, and 9). The lateral expansion of the nonlinearity is indeed established immediately through a fast component of contrast adaptation (Victor, 1987), but as shown here, that is accompanied by a substantial

depolarization (Figure 7B), which is counteracted only in the course of subsequent slow adaptation. This depolarization will certainly affect ganglion cell spiking (Figure 8). Therefore, when contrast changes rapidly within the scene, or during the immediate response to moving objects, retinal processing will not behave as though stimulus fluctuations were simply scaled in magnitude.

Slow Adaptation to a Contrast Change

During the tens of seconds following an increase in contrast, there is further significant change in retinal output: ganglion cells continue to respond to the same features in the visual stimulus, but with progressively fewer spikes as contrast adaptation proceeds (Figure 3C). Thus, the message conveyed by individual spikes changes little during this period, but the ganglion cell produces fewer of them. A similar separation between a rapid change in the meaning of spikes, and a subsequent slow change in firing rate has been documented for neural coding in the fly retina (Fairhall et al., 2001).

In several retinal cell types, the most prominent effect of slow contrast adaptation is a gradual shift in the baseline membrane potential (Figures 5–7 and 9). By comparison, the kinetics of the light response, as expressed in the temporal filter of the LN model, are established within 0.2 s of the contrast step and then remain unchanged. Similarly, the nonlinearity of the light response—which reflects the effects of rectification, thresholding, and saturation in the synaptic circuits—remains largely unchanged in shape.

In ganglion cells, the time course of the slow hyperpolarization after a contrast step mirrors the slow decline in their firing rate (Figure 7D). Moreover, injecting hyperpolarizing current into a ganglion cell, without any change in stimulus contrast, produced a decrease in sensitivity very similar to that of slow contrast adapta-
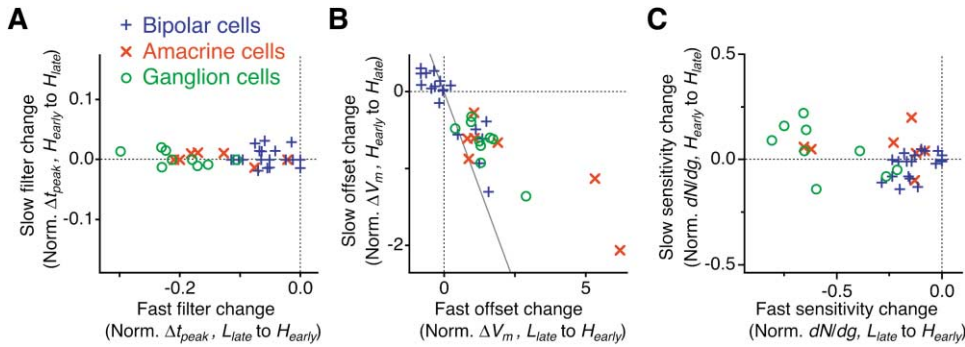
Figure 9. Changes in Kinetics, Baseline Membrane Potential, and Sensitivity during Fast and Slow Adaptation

For each bipolar cell, adapting amacrine cell and ganglion cell, changes in LN models during slow adaptation, between H_{early} and H_{late}, are plotted against changes during fast adaptation, between L_{late} and H_{early}.

(A) The fractional change in time to peak (Δt_{peak}) of the filter between H_{early} and H_{late} compared to Δt_{peak} between L_{late} and H_{early}.

(B) The shift in membrane potential compared during slow and fast adaptation. Both numbers are normalized for each cell as in Figure 5G by the standard deviation of the membrane potential (V_{sd}) during H_{late}. The diagonal line is the negative of the identity, indicating that in general, the slow shift did not compensate completely for the fast shift.

(C) Fractional change in sensitivity between H_{early} and H_{late} compared to the change between L_{late} and H_{early}. The change in sensitivity between two stimulus periods was calculated as the difference in the slopes of the nonlinearity, dN/dg, averaged over those values of g common to both conditions, and normalized to the slope in L_{late} (fast change) or H_{early} (slow change).

tion (Figure 8). Thus, it appears likely that the slow adaptation observed in the retinal output signals derives from a gradual hyperpolarization of the ganglion cell membrane.

Throughout the retinal circuit there was a strict relation between fast and slow contrast adaptation: every neuron that experienced a fast polarization of the membrane potential after the contrast switch also showed subsequent slow adaptation. More importantly, the slow process always counteracted the fast offset of the baseline (Figure 9). This held true for both depolarizing and hyperpolarizing shifts. The slow change in membrane potential thus acts like a homeostatic correction to the initial effects of the contrast step.

The effects of this slow compensation might be transmitted between neurons, for example, if hyperpolarization of bipolar cells reduces transmitter release to amacrine and ganglion cells, in turn hyperpolarizing these postsynaptic cells. Alternatively, slow adaptation might occur via negative feedback within each individual neuron. In mammalian visual cortex, pyramidal cells undergo shifts in the membrane potential during slow contrast adaptation (Carandini and Ferster, 1997). In motion-sensitive neurons of the fly visual system, baseline shifts occur during slow adaptation to moving stimuli (Harris et al., 2000). In both cases, it appears that an activity-dependent K^+ conductance serves the homeostatic feedback, producing a hyperpolarization when a step increase in excitatory input raises intracellular levels of Na^+ (Sanchez-Vives et al., 2000) or Ca^{2+} (Harris et al., 2000). Retinal bipolar cells contain a prominent Ca^{2+}-dependent K^+ conductance (Burrone and Lagnado, 1997; Kaneko and Tachibana, 1985), and a recent study showed that buffering Ca^{2+} in OFF-type bipolar cells interferes with contrast adaptation (Rieke, 2001).

If individual retinal interneurons do indeed perform contrast adaptation independently, a number of additional phenomena could be explained. For example, slow contrast adaptation can increase the sensitivity of

a ganglion cell to high spatial frequencies, while at the same time decreasing its sensitivity to low frequencies, which led Smirnakis et al. (1997) to postulate multiple sites of adaptation. Slow adaptation in individual bipolar cells would explain why contrast adaptation can occur on a fine spatial scale, smaller than the ganglion cell receptive field (Brown and Masland, 2001). It also accounts for the observation that blockers of amacrine cell transmission in the retina do not eliminate contrast-dependent changes in sensitivity (Brown and Masland, 2001; Rieke, 2001). Finally, adaptation originating in different cell types may well follow a different time course. This would explain why the responses of ganglion cells, which are affected by all these events, show a mixture of time scales for slow contrast adaptation (Figures 1E and 7D) (Brown and Masland, 2001; Kim and Rieke, 2001), whereas in bipolar cells there appears to be only one (Rieke, 2001). In addition, adaptation to a contrast increase is generally faster than to a decrease (DeWeese and Zador, 1998; Kim and Rieke, 2001; Smirnakis et al., 1997). This might reflect differences in the time course of Ca^{2+} entry and removal.

In summary, fast and slow contrast adaptation modulate retinal circuitry in very different ways. In fact, on a cellular level, the slow adaptation appears to counteract the fast membrane polarization experienced during fast adaptation. At the output of the retina, fast adaptation alters temporal processing and stimulus sensitivity, whereas slow adaptation modulates the strength of a ganglion cell's firing.

Modeling and Outlook
The present work used the LN model to summarize a neuron's response to an arbitrary stimulus. It is generally appreciated that explicit mathematical models are needed to test quantitative hypotheses. However, in a more fundamental way, these models also serve to define the vocabulary by which we discuss neural responses. For example, the "kinetics of the light response" is defined

classically as "the time course of the response to a flash of light." This comes with an implied assumption that the system integrates its inputs linearly; otherwise, the flash response would be useless for predicting the response to any other stimulus. By making that assumption explicit in form of an LN model, one can define "kinetics" more precisely as "the time course of the linear filter." Other common terms like "sensitivity," "threshold," or "saturation" also derive from an LN model, referring to the slope, the foot, or the knee of the nonlinearity. Thus the LN model is a rather common implicit picture of system function, both in sensory neurophysiology and psychophysics.

In this context and in our present usage, "adaptation" simply means a change in the parameters of the LN model. "Contrast adaptation" are changes in the LN model triggered by a sudden change in stimulus contrast. As the term is somewhat model dependent, its meaning may well change when the default models change. For example, Victor (1987) augmented the LN model with a nonlinear feedback loop, the "contrast gain control," which successfully predicts the fast change in kinetics and gain of ganglion cell spiking immediately upon a contrast switch. If one adopts this model for the light response, then there is no fast change of parameters, only the subsequent slow adaptation. One expects that the future will bring a model of visual processing that also predicts successfully the slow changes using the history of the stimulus, and thus makes explicit the rules governing both the immediate light response and its adaptation over multiple time scales.

Experimental Procedures

Electrophysiology
To record the spike trains of retinal ganglion cells, the isolated retina of a tiger salamander or rabbit was placed on a flat array of 61 microelectrodes as described (Meister et al., 1994; Smirnakis et al., 1997) and bathed in oxygenated Ringer's solution at 20°C–22°C (salamander) or Ames medium at 37°C (rabbit). The firing rate of ganglion cells during steady-state high contrast (H_{late}) was 4 ± 1 Hz (n = 15) for salamander and 9 ± 2 Hz (n = 11) for rabbit.

For simultaneous intracellular recording from salamander retinas using sharp microelectrodes, the retina was held in place under a layer of 0.5% agarose (Type III-A: High EEO, Sigma) of ∼100 μm thickness, with a dialysis membrane containing several 150–300 μm holes. Intracellular electrodes were positioned over the retina under infrared illumination, viewed through an IR-sensitive CCD camera, and guided through the dialysis membrane and agarose into the retina. Electrodes were filled with 2 M potassium acetate and either 2% Alexa Fluor 488 or 5% Rhodamine Dextran 10,000 MW (Molecular Probes), with a final impedance of 150–250 MΩ.

Intracellular recordings were made from six cone photoreceptors (resting membrane potential −41 ± 2mV, mean ± SEM), 7 horizontal cells (−47 ± 3mV), 18 bipolar cells (−40 ± 2mV), 26 amacrine cells (−52 ± 2mV), and 12 ganglion cells (−64 ± 2mV). Adapting cells had resting potentials similar to those that did not adapt: slowly adapting bipolar cells, −41 ± 3mV, n = 11; bipolar cells that did not slowly adapt, −39 ± 3mV, n = 7; adapting amacrine cells, −51 ± 5mV, n = 8; and nonadapting amacrine cells, −52 ± 2mV, n = 18.

Recordings used to produce LN models ranged from 5 to 30 min in duration. Light responses were stable in amplitude over this time period. In many cases, recordings were of sufficient length to map receptive fields using white noise stimuli for 5–10 min (data not shown). After recording, cells were filled iontophoretically (−1 to −5 nA pulses, ∼10–15 min) and imaged using a confocal microscope with a ×40 oil-immersion objective.

Visual Stimulation
Spatially uniform white light was projected onto the retina from a video monitor, at a photopic mean intensity of ∼10 mW/m². A new stimulus intensity was chosen every 30 ms from a Gaussian probability distribution with mean intensity M and standard deviation W (Smirnakis et al., 1997). Contrast, defined as W/M, was 0.35 for high-contrast flicker, and 0.05 for low-contrast flicker. By keeping the mean light intensity constant throughout the experiment, we avoided any contributions from light adaptation.

Analysis
The stimulus intensity $s(t)$ was normalized to have zero mean, a standard deviation equal to the contrast, and dimensionless units. The filter $F(t)$ was 1 s in duration and was computed as the correlation between $s(t)$ and the response $r(t)$, normalized by the autocorrelation of the stimulus. In the Fourier domain,

$$\tilde{F}(\omega) = \frac{\langle \tilde{s}^*(\omega)\tilde{r}(\omega)\rangle}{\langle \tilde{s}^*(\omega)\tilde{s}(\omega)\rangle}, \tag{1}$$

where $\tilde{s}(\omega)$ is the Fourier transform of $s(t)$, $\tilde{s}^*(\omega)$ its complex conjugate, and $\langle\cdots\rangle$ denotes averaging over 1 s segments spaced every 0.1 s throughout the recording. For perfect Gaussian white noise, the optimal linear filter is given by the numerator of Equation 1 (Hunter and Korenberg, 1986), and the denominator is identically 1. Light delivered by a video monitor is not perfectly uncorrelated in time (Keat et al., 2001), and the denominator helps correct for these deviations.

This calculation was performed separately in various time windows surrounding the contrast switch, defined in Figure 1E, and the results averaged over multiple 60 s trials. For the very short interval $H_{0.1-0.2}$, the filter was calculated in the time domain by reverse correlation of the spikes in that interval to the stimulus (Smirnakis et al., 1997), and restricted to 0.2 s length. The amplitude of the filter was normalized as explained below.

The stimulus was convolved with the filter, by computing

$$g(t) = \int F(\tau)s(t - \tau)d\tau. \tag{2}$$

Then, the fixed nonlinearity $N(g)$ was calculated by plotting $r(t)$ against $g(t)$ and averaging the values of r over bins of g containing an equal number of points. Finally, the prediction of the LN model was calculated as

$$r'(t) = N(g(t)) = N(\int F(\tau)s(t - \tau)d\tau). \tag{3}$$

As can be inferred from Equation 3, an ambiguity exists in the parameters of the LN model: expanding the amplitude of the filter $F(\tau)$ or compressing the g axis of the nonlinearity $N(g)$ by the same factor yields precisely the same predicted response, $r'(t)$. We chose to scale the filter in amplitude so that the variance of the filtered stimulus, $g(t)$, was equal to the variance of the stimulus, $s(t)$:

$$\int g^2(\tau)d\tau = \int s^2(\tau)d\tau. \tag{4}$$

With this convention, if a neuron changes its sensitivity to the stimulus without altering its kinetics, the change will appear exclusively in the shape of the nonlinearity $N(g)$. Thus, $F(t)$ summarizes temporal processing, and $N(g)$ captures the sensitivity to the stimulus.

To analyze the subthreshold membrane potential of ganglion cells, spikes were detected by setting a threshold for the derivative of the membrane potential, and then digitally removed by interpolation between adjacent points of the waveform. For fitting of the ganglion cell spiking response, spike trains were converted into a continuous firing rate by binning the spike times in 1 ms intervals.

The normalized root-mean-square difference between two filters, $F_1(t)$ and $F_2(t)$, was calculated as

$$\sqrt{2\frac{\int (F_1(t) - F_2(t))^2 dt}{\int (F_1(t)^2 + F_2(t)^2)dt}}. \tag{5}$$

Differences between nonlinearities $N(g)$ were calculated in the same manner. For calculating the rms difference between predicted and

actual spiking responses, spike trains were smoothed using a Gaussian time window with 10 ms standard deviation.

References

Barlow, H.B., and Levick, W.R. (1969). Changes in the maintained discharge with adaptation level in the cat retina. J. Physiol. *202*, 699–718.

Baylor, D.A., Fuortes, M.G., and O'Bryan, P.M. (1971). Receptive fields of cones in the retina of the turtle. J. Physiol. *214*, 265–294.

Berry, M.J., and Meister, M. (1998). Refractoriness and neural precision. J. Neurosci. *18*, 2200–2211.

Berry, M.J., Warland, D.K., and Meister, M. (1997). The structure and precision of retinal spike trains. Proc. Natl. Acad. Sci. USA *94*, 5411–5416.

Berry, M.J., 2nd, Brivanlou, I.H., Jordan, T.A., and Meister, M. (1999). Anticipation of moving stimuli by the retina. Nature *398*, 334–338.

Blakemore, C., and Campbell, F.W. (1969). On the existence of neurones in the human visual system selectively sensitive to the orientation and size of retinal images. J. Physiol. *203*, 237–260.

Brown, S.P., and Masland, R.H. (2001). On the spatial scale and cellular substrate of contrast adaptation by retinal ganglion cells. Nat. Neurosci. *4*, 44–51.

Burrone, J., and Lagnado, L. (1997). Electrical resonance and Ca^{2+} influx in the synaptic terminal of depolarizing bipolar cells from the goldfish retina. J. Physiol. *505*, 571–584.

Carandini, M., and Ferster, D. (1997). A tonic hyperpolarization underlying contrast adaptation in cat visual cortex. Science *276*, 949–952.

Chander, D., and Chichilnisky, E.J. (2001). Adaptation to temporal contrast in primate and salamander retina. J. Neurosci. *21*, 9904–9916.

Chichilnisky, E.J. (2001). A simple white noise analysis of neuronal light responses. Network *12*, 199–213.

DeWeese, M., and Zador, A. (1998). Asymmetric dynamics in optimal variance adaptation. Neural Comput. *10*, 1179–1202.

Enroth-Cugell, C., and Lennie, P. (1975). The control of retinal ganglion cell discharge by receptive field surrounds. J. Physiol. *247*, 551–578.

Fairhall, A.L., Lewen, G.D., Bialek, W., and van Steveninck, R.R.D. (2001). Efficiency and ambiguity in an adaptive neural code. Nature *412*, 787–792.

Greenlee, M.W., Georgeson, M.A., Magnussen, S., and Harris, J.P. (1991). The time course of adaptation to spatial contrast. Vision Res. *31*, 223–236.

Harris, R.A., O'Carroll, D.C., and Laughlin, S.B. (2000). Contrast gain reduction in fly motion adaptation. Neuron *28*, 595–606.

Hunter, I.W., and Korenberg, M.J. (1986). The identification of nonlinear biological systems: Wiener and Hammerstein cascade models. Biol. Cybern. *55*, 135–144.

Kaneko, A., and Tachibana, M. (1985). A voltage-clamp analysis of membrane currents in solitary bipolar cells dissociated from Carassius auratus. J. Physiol. *358*, 131–152.

Keat, J., Reinagel, P., Reid, R.C., and Meister, M. (2001). Predicting every spike: a model for the responses of visual neurons. Neuron *30*, 803–817.

Kim, K.J., and Rieke, F. (2001). Temporal contrast adaptation in the input and output signals of salamander retinal ganglion cells. J. Neurosci. *21*, 287–299.

MacNeil, M.A., Heussy, J.K., Dacheux, R.F., Raviola, E., and Masland, R.H. (1999). The shapes and numbers of amacrine cells: matching of photofilled with Golgi-stained cells in the rabbit retina and comparison with other mammalian species. J. Comp. Neurol. *413*, 305–326.

Meister, M., Pine, J., and Baylor, D.A. (1994). Multi-neuronal signals from the retina: acquisition and analysis. J. Neurosci. Methods *51*, 95–106.

Ohzawa, I., Sclar, G., and Freeman, R.D. (1985). Contrast gain control in the cat's visual system. J. Neurophysiol. *54*, 651–667.

Pugh, E.N., Nikonov, S., and Lamb, T.D. (1999). Molecular mechanisms of vertebrate photoreceptor light adaptation. Curr. Opin. Neurobiol. *9*, 410–418.

Rieke, F. (2001). Temporal contrast adaptation in salamander bipolar cells. J. Neurosci. *21*, 9445–9454.

Sakai, H.M., and Naka, K. (1987). Signal transmission in the catfish retina. V. Sensitivity and circuit. J. Neurophysiol. *58*, 1329–1350.

Sakai, H.M., Naka, K., and Korenberg, M.J. (1988). White-noise analysis in visual neuroscience. Vis. Neurosci. *1*, 287–296.

Sakai, H.M., Wang, J.L., and Naka, K. (1995). Contrast gain control in the lower vertebrate retinas. J. Gen. Physiol. *105*, 815–835.

Sanchez-Vives, M.V., Nowak, L.G., and McCormick, D.A. (2000). Cellular mechanisms of long-lasting adaptation in visual cortical neurons in vitro. J. Neurosci. *20*, 4286–4299.

Shapley, R.M., and Victor, J.D. (1978). The effect of contrast on the transfer properties of cat retinal ganglion cells. J. Physiol. *285*, 275–298.

Smirnakis, S.M., Berry, M.J., Warland, D.K., Bialek, W., and Meister, M. (1997). Adaptation of retinal processing to image contrast and spatial scale. Nature *386*, 69–73.

Truchard, A.M., Ohzawa, I., and Freeman, R.D. (2000). Contrast gain control in the visual cortex: monocular versus binocular mechanisms. J. Neurosci. *20*, 3017–3032.

Victor, J.D. (1987). The dynamics of the cat retinal X cell centre. J. Physiol. *386*, 219–246.

Warland, D.K., Reinagel, P., and Meister, M. (1997). Decoding visual information from a population of retinal ganglion cells. J. Neurophysiol. *78*, 2336–2350.

Wu, S.M., Gao, F., and Maple, B.R. (2000). Functional architecture of synapses in the inner retina: segregation of visual signals by stratification of bipolar cell axon terminals. J. Neurosci. *20*, 4462–4470.

Yang, X.L., and Wu, S.M. (1996). Response sensitivity and voltage gain of the rod- and cone-horizontal cell synapses in dark- and light-adapted tiger salamander retina. J. Neurophysiol. *76*, 3863–3874.

Yang, J., and Stevenson, S.B. (1999). Post-retinal processing of background luminance. Vision Res. *39*, 4045–4051.

Yang, C.Y., Lukasiewicz, P., Maguire, G., Werblin, F.S., and Yazulla, S. (1991). Amacrine cells in the tiger salamander retina: morphology, physiology, and neurotransmitter identification. J. Comp. Neurol. *312*, 19–32.